Direct observation of non-Gaussian distribution of local magnetic properties in ferromagnetic thin films

Sug-Bong Choe and Sung-Chul Shin
Department of Physics and Center for Nanospinics of Spintronic Materials, Korea Advanced Institute of Science and Technology, Taejon 305-701, Korea
(Received 27 March 2002; published 7 June 2002)

We report our experimental finding that magnetic properties of Co-based multilayer films are shown to exhibit their local variations far from the Gaussian (or Lorentzian) distribution which are usually assumed. The local variations of the coercivity and the field dependence $\lambda(=-\partial \ln \tau/\partial H)$ were determined from measurements of the hysteresis loop and the field-dependent switching time τ, respectively, on spatially resolved local regions 400 nm in size by means of a magneto-optical microscope magnetometer. We show that the two local magnetic properties inversely correlate with each other and a thermally activated process takes place during magnetization reversal on a submicrometer scale in ferromagnetic thin films.

DOI: 10.1103/PhysRevB.65.224424 PACS number(s): 75.70.Ak, 07.55.Jg, 68.60.Dv, 75.60.Lr

In general, the magnetic properties of ferromagnetic thin films are spatially inhomogeneous because of structural and/or chemical imperfections inevitably introduced in the film preparation process.[1–4] Due to the lack of available techniques capable of providing detailed information about the variations with a high spatial resolution, the variations are typically considered under an assumption of the Gaussian (or Lorentzian) distribution in most theoretical approaches—for instance, Preisach and micromagnetic modeling.[4–6] However, there is no clear physical reason for this. The question on the variations in real films is fundamentally important for exploring a realistic model of the magnetic domain configuration and reversal dynamics, which are known to be sensitive to local magnetic properties as evidenced from recent observations—for instance, for Co films grown on Au(111),[1] Pt/Co/Pt(111) trilayers,[2] and Co/Pd multilayers.[3] It is also a crucial technological issue in achieving a high performance of magnetic information technology,[7–9] in which the information is stored in the form of magnetic domains.

Versatile experimental techniques including magnetic force microscopy (MFM),[10] scanning electron microscopy with polarization analysis (SEMPA),[11] spin-polarized low-energy electron microscopy (SPLEEM),[12] near-field scanning optical microscopy (NSOM),[13] and spin-polarized scanning tunneling microscopy (SPSTM) (Ref. 14) have been developed to investigate microscopic domain structures with a spatial resolution of some tens of nanometers. But despite the high spatial resolution of these techniques, quantitative measurements of the local magnetic properties relating to domain reversal behavior have not yet been developed because of limitations imposed by the impossibility of applying a magnetic field and/or slow data acquisition time. On the other hand, the magneto-optical Kerr effect (MOKE) has been utilized to characterize dynamic properties such as the activation volume and the hysteresis loop by using either a focused laser beam or an optical microscope equipped with a charge-coupled device (CCD) camera.[15–17] However, these measurement techniques basically focused on the whole area of a film or a single local area of the patterned sample.

Hence, to date simultaneous local probing of the magnetic properties relating to domain reversal behavior with a high spatial resolution remains a scientific challenge. In this article, we present a technique for the simultaneous probing of local magnetic properties on a submicrometer scale by means of a magneto-optical microscope magnetometer (MOMM) and report our experimental finding that the local variations of the coercivity and the field dependence in Co-based multilayer films are far from the Gaussian (or Lorantzian) distribution. Here, the field dependence λ is defined as $\lambda = -\partial \ln \tau/\partial H$, where τ is the switching time. The field dependence closely relates to the activation volume. For example, it can be essentially given by the product of the activation volume times the saturation magnetization in a uniform film. However, for films exhibiting the local irregularities of the present study, it is hard to distinguish the effects between local variations from the activation volume and the saturation magnetization. Thus, here we present the field dependence as a quantity directly determined from experiments with fewer assumptions.

The MOMM system mainly consists of an optical polarizing microscope capable of magnetic domain imaging by utilizing the magneto-optical Kerr effect.[3,18] A CCD camera captures the domain image in the form of an array of Kerr intensity measured from CCD pixels with a spatial resolution of 400 nm. By storing the domain images and tracing the Kerr intensity variation for every individual CCD pixel, it is possible to obtain (1) an array of local Kerr hysteresis loops while sweeping the external magnetic field from an electromagnet, as well as (2) an array of magnetization viscosity curves during magnetization reversal under a constant applied magnetic field. We stress that all the hysteresis loops and viscosity curves are simultaneously obtained for every CCD pixel in each run; this enables us to avoid measurement errors from different runs as well as the magnetic aftereffect due to a long measurement time. The most striking feature of the present system is the fact that we can directly map the local distribution of magnetic properties such as the coercivity, switching time, and field dependence, respectively. Therefore, the local variations of the magnetic properties can be directly compared with each other to search for any possible correlations between them. The ability of spatially resolved probing on magnetic properties enables us not only to

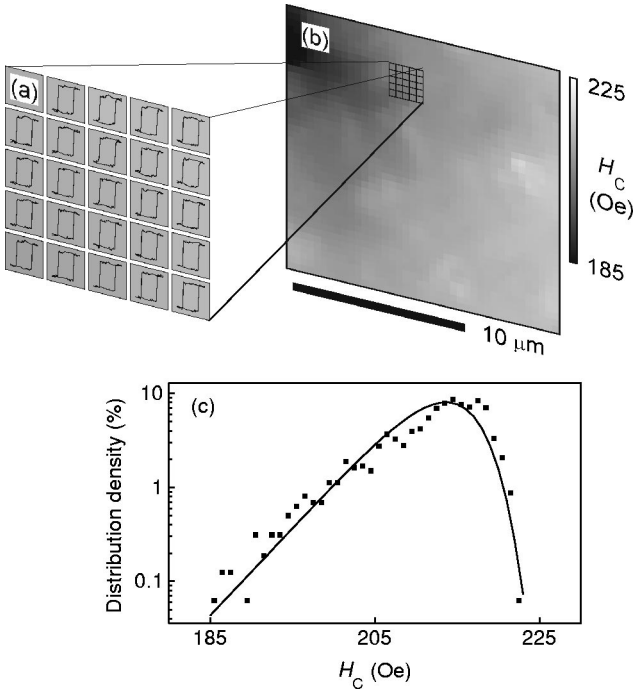

FIG. 1. (a) Typical hysteresis loops measured from each corresponding local region of 400×400 nm^2 on a (2.5-Å Co/11-Å Pd)$_5$ sample, where the *x* axis is an applied field ranging from -0.4 to 0.4 kOe and the *y* axis is the normalized Kerr angle. (b) Distribution map of the local coercivity generated from the simultaneous probing of the local hysteresis loops. (c) Distribution density of the local coercivity from the sample shown in (b), where the density was obtained for every 1-Oe interval. The solid line shows the best fit using Eq. (3).

determine their real distributions, but also to obtain an in-depth understanding of domain reversal dynamics.

To characterize the local variation of the magnetic properties in ferromagnetic thin films, Co-based multilayer samples were chosen because we could produce various magnetic and/or structural properties by varying the layer thickness and repeats. In addition, they are of current technological interest as a high-density magnetic information medium because of their large Kerr effect; this made our experiment much easier for fine-scale domain imaging. A number of Co/Pd and Co/Pt multilayer samples with various multilayer structures were prepared on glass substrates under a base pressure of 2.0×10^{-7} Torr at ambient temperature. Low-angle x-ray diffraction studies using Cu $K\alpha$ radiation revealed that all samples showed distinct peaks indicating an existence of the multilayer structure. High-angle x-ray diffraction studies showed that the samples grew along a [111] cubic orientation. All samples in this study had perpendicular magnetic anisotropy and showed square Kerr hysteresis loops.

Using the MOMM, we indeed probed the local variations of the magnetic properties of the Co-based multilayer films. Figure 1 demonstrates the local coercivity variation of a (2.5-Å Co/11-Å Pd)$_5$ multilayer film. For illustration, the typical hysteresis loops are depicted in each box of Fig. 1(a). The shape of the hysteresis loops appears to be same, but a close examination reveals that the value of the coercivity varies slightly. For clear visualization, we filled each box with the color corresponding to the magnitude of the coercivity. Mapping the colors onto a two-dimensional plane, we generated the spatial distribution map of the local variation as shown in Fig. 1(b). The coercivity distribution was confirmed to be the same for a number of different measurements for a given sample. However, the distribution among the samples having different multilayer structure was quite contrasting. For instance, the coercivity variation became rougher with increasing repeats of layers among the samples.[3] This might be explained by the fact that the coercivity is sensitive to the microstructural irregularities accumulating with increasing interfaces.[19–21] Antiferromagnetic (AFM) studies indeed revealed a tendency toward larger surface roughness with increasing repeats. We also observed a similar dependence in the Co/Pt multilayer samples by changing the multilayer structure.

Surprisingly, our experimental results directly show that the coercivity distribution is far from the Gaussian (or Lorentzian) distribution. In Fig. 1(c), we illustrate the distribution density of the local coercivity of the sample shown in Fig. 1(b). The non-Gaussian distribution might come from the magnetic interaction between the nonisolated local regions in ferromagnetic thin films via the exchange and magnetostatic coupling, which results in a situation different from the case of an isolated random phenomenon revealing the Gaussian distribution. Also, it closely relates to the energy barrier distributions of the wall-pinning and nucleation processes during magnetization reversal. The asymmetric shape has already been considered in the Preisach approach, but the detailed shape of the distribution density was far from any well-known theoretical models, such as the log-normal–Gaussian and factorized Lorentzian distributions:[5] Serious deviations were found for the two distribution models at either the low or high regimes, respectively.

To quantitatively understand the asymmetric distribution density, we utilized the dynamical magnetization equation developed by Raquet *et al.*[22] to calculate a major hysteresis loop by considering both the wall-motion and nucleation processes. The normalized magnetization *m* in the equation is given as a function of the sweeping magnetic field *H* by

$$m(H)=1-2\exp\left[-2\alpha k^2\left\{(1-e^{\xi})\left(1-\frac{1}{k}+\frac{1}{2k^2}\right)+\xi\left(1-\frac{1}{k}\right)+\frac{\xi^2}{2}\right\}\right], \tag{1}$$

where $\xi=\xi(H)=R_0\exp(-\lambda H_0)[1-\exp(\lambda H)]/\lambda\dot{H}$, introducing the following physical parameters:

$$\text{sweeping rate}\quad \dot{H}=dH/dt,$$

$$\text{field dependence}\quad \lambda=M_S V_A/k_B T,$$

$$\text{reversal parameter}\quad k=V_0/r_c R_0,$$

$$\text{nucleation site coverage}\quad \alpha. \tag{2}$$

TABLE I. The values of the magnetic properties used in calculation, where M_S was measured by a vibrating sample magnetometer (VSM) and V_A was estimated from the field dependence of the magnetization reversal (Ref. 3). V_0 and R_0 were determined based on the time-resolved domain evolution patterns under reversing magnetic field H_0 (Ref. 18), respectively. r_c is given by the radius of the activation volume as $r_c=(V_A/\pi t_f)^{1/2}$, where t_f is the film thickness.

Magnetic properties	Values
Saturation magnetization M_S (emu/cm^3)	288
Activation volume V_A (cm^3)	1.06×10^{-17}
Field dependency λ (1/Oe)	7.4×10^{-2}
Sweeping rate $\dot{H}$ (Oe/s)	10
Applied field H_0 (Oe)	150
Wall-motion speed V_0 (cm/s)	1.9×10^{-6}
Nucleation rate R_0 (1/s)	5.1×10^{-6}
Characteristic radius r_c (cm)	2.2×10^{-6}
Reversal parameter k	1.6×10^{5}
Nucleation site coverage α	0.26

Here, M_S is the saturation magnetization, V_A is the activation volume, k_B is Boltzmann's constant, T is the temperature, and r_c is the characteristic radius of nucleated domains, respectively. Here, V_0 and R_0 are the wall-motion speed and nucleation rate triggered by applying a constant magnetic field H_0 near the coercivity, respectively. The nucleation site coverage α is the fraction of the area of the nucleation sites over the total area under examination. Then, the coercivity distribution is obtained by

$$\sigma(H)=[m(H+\Delta H/2)-m(H-\Delta H/2)]/\Delta H, \qquad (3)$$

where ΔH is the field step for generating the distribution. Remarkably, the local coercivity distribution is well explained using this function as shown by the solid line in Fig. 1(c). Note that experimentally measured values of the physical parameters as listed in Table I were used in obtaining the theoretical curve, except the nucleation site coverage chosen for the best fit. The r_c was found to be nearly same as the minimum stable domain size or the domain wall width in uniform Co-based multilayer film, which have been believed to be a few tens of a nanometer. However, for polycrystalline films, r_c might be much larger than the domain wall width at the polycrystalline grain boundary where the domain wall width shrinks due to a less exchange stiffness. We would like to mention that the distribution densities of all the other Co/Pd and Co/Pt multilayer samples were confirmed to be well characterized using this function. We found that the lower bound of the distribution was determined by the counterbalance between the finite wall-motion speed and the field-sweeping time, while the higher bound was ascribed to domain coalescence. The minor deviation between the experimental data and the theoretic curve is believed to be ascribed to the local magnetic variation. It should be mentioned that a consistent result was also obtained by two-dimensional micromagnetic simulation[18] using precisely the same magnetic properties.

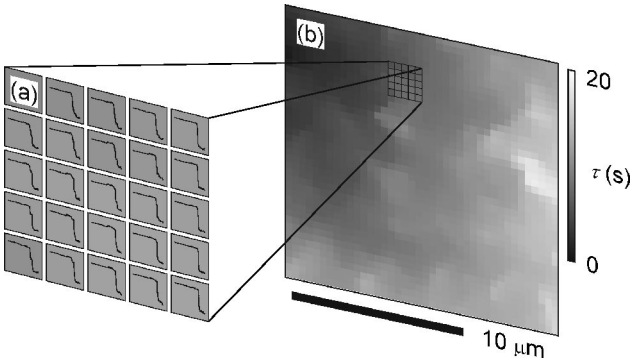

FIG. 2. (a) Typical viscosity curves measured from each corresponding local region shown in Fig. 1, where the x axis is the elapsed time in a logarithmic scale with a range from 0.2 to 20 s and the y axis is the normalized Kerr angle. The curves were obtained under a constant magnetic field of 196 Oe, which corresponded to an approximately 90% mean coercivity. (b) Distribution map of the local switching time generated from the simultaneous probing of the local viscosity curves.

A fundamental question then is how the coercivity variation affects magnetization reversal dynamics. For this purpose, a reversal experiment starting from a saturated state was carried out by means of time-resolved observation of domain evolution, triggered by applying a constant reversed magnetic field.[4,18,23] Figure 2 demonstrates the domain evolution pattern at precisely the same position of the sample as shown in Fig. 1. We generated the distribution map shown in Fig. 2(b) by mapping the local switching time determined from the corresponding magnetization viscosity curve shown in Fig. 2(a). The map clearly shows that the switching time is also locally nonuniform on a submicrometer scale. In this sample, domain reversal proceeds by the wall-motion process from a nucleation site; the smooth variation of the switching time indicates a gradual expansion of domain via a continuous wall-motion process from the nucleation site, whereas the nonisotropic expansion evidences the spatial inhomogenuity in the magnetic properties.[22–24] Most importantly, the domain evolution pattern is truly coincident with the coercivity distribution shown in Fig. 1(b); this coincidence was observed for all other samples. This directly demonstrates the existence of a close correlation between the coercivity distribution and domain reversal dynamics.

Crucial information on the dynamic properties was obtained from the magnetic field dependence of the switching time.[25] We measured an array of the field dependence of the local regions by tracing the switching time at every corresponding pixel under various applied magnetic fields. The field dependence of the switching time is illustrated in each box of Fig. 3(a), where the x axis is an applied magnetic field in a linear scale and the y axis is the switching time in a logarithmic scale. We clearly see from each box that the switching time depends exponentially on the applied magnetic field. The exponential dependence could be analyzed within the context of a thermally activated relaxation process

$$\tau=\tau_0\exp[\lambda(H_C-H)], \qquad (4)$$

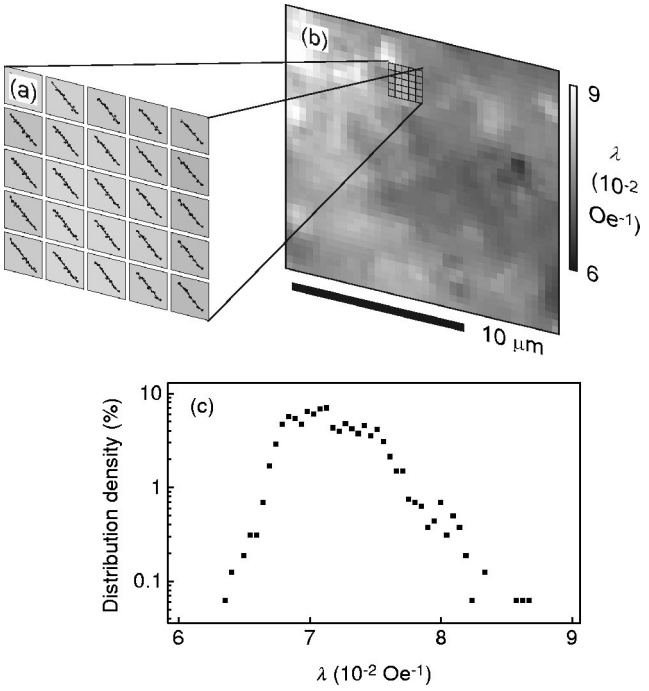

FIG. 3. (a) Typical field dependence measured from each corresponding local region shown in Fig. 1, where the *x* axis is an applied field ranging from 150 to 200 Oe and the *y* axis is the switching time in a logarithmic scale ranging from 1 to 100 s. The solid line in each box represents the best fit using Eq. (4). (b) Distribution map of the local field dependence generated from the simultaneous probing of the local field dependence. (c) Distribution density of the local field dependence from the sample shown in (b), where the density was obtained for every $5\times10^{-3}\,\mathrm{Oe}^{-1}$ interval.

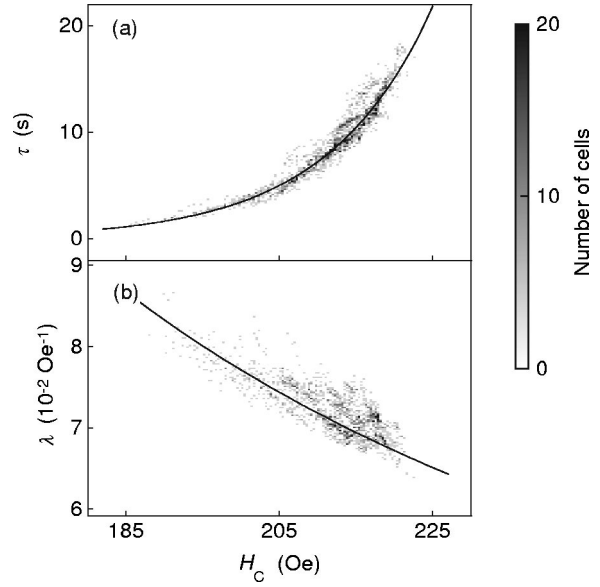

FIG. 4. (a) Correlated distribution between the coercivity H_C in Fig. 1 and switching time τ in Fig. 2. The solid line represents the best fit using Eq. (4). (b) Correlated distribution between the coercivity H_C in Fig. 1 and field dependence λ in Fig. 3. The solid line is a guide to the eye of an inverse proportionality.

where τ_0 is the characteristic switching time for the coercivity H_C.[23,25] The equation is derived from the Neél-Brown model[26,27] assuming a first-order uniaxial anisotropy by linear expansion of the energy barrier with H near the mean coercivity. The clear exponential dependence for every local region directly demonstrates that a thermally activated magnetization reversal process takes place, respectively, on local regions of a submicrometer scale in ferromagnetic thin films. It is worthwhile to mention that we could determine the local field dependence λ from the best fit using Eq. (4). Mapping the values, we generated the local variation map of the field dependence shown in Fig. 3(b). The figure vividly shows the spatial fluctuation of the local field dependence. The values of the field dependence were confirmed to be essentially same in several repeated measurements. The distribution of the field dependence is again observed to be neither Gaussian nor Lorentzian, as seen in Fig. 3(c). To the best of our knowledge, this is the first time that the nonuniform distribution of the field dependence on a submicrometer scale has been probed.

The field dependence is closely related to the activation magnetic moment $M_S V_A$, which characterizes the basic magnetic moment acting as a single magnetic particle during magnetization reversal. Note that the field dependence λ in Eq. (2) is intrinsically given by $M_S V_A/k_B T$ for an isolated particle considering first-order uniaxial anisotropy. On the other hand, the field dependence in real continuous films is determined not only by its intrinsic nature but also by interaction with the magnetization states of neighbor regions. For instance, the sample showing a wall-motion dominant magnetization reversal exhibits a smooth gradient in the spatial distribution of the field dependence as revealed in Fig. 3(b); this gradient is possibly caused by domain propagation from neighbor regions rather than by the smooth change in the intrinsic magnetic properties. It was indeed confirmed by a micromagnetic simulation that a smooth gradient in the spatial distribution of the field dependence takes place around a nucleation site, even though the intrinsic magnetic properties of the region are identical. However, though it is not an intrinsic property, it should be mentioned that the field-dependent switching behavior is inherently reproduceable on any local regions in a given sample.

The most striking fact is that all the local variations of the magnetic properties correlate with each other. For a quantitative analysis, we measured the correlated distributions among the magnetic quantities. First, we measured the number of pixels having the corresponding values of coercivity and switching time. Figure 4(a) illustrates the correlated distribution in H_C-τ coordinates. In the figure, we clearly see that the switching time correlates with the coercivity. The excellent correlation evidences a definite effect of the local coercivity variation on the local switching time during magnetization reversal.[3] Note that the correlation can be well described by a thermally activated relaxation process, as denoted by the solid line of the best fit using Eq. (4). This again demonstrates that a thermally activated process governs magnetization reversal of the local regions. We also see a correlation between the field dependence and coercivity. In Fig. 4(b), we illustrate the correlated distribution in H_C-λ coordinates. The figure shows that the field dependence in-

versely correlates with the coercivity, as shown by a solid line of the best fit. The inverse proportionality possibly comes from the contribution of the anisotropy field, which is known to be inversely proportional to the magnetization.

In conclusion, we report the experimental finding that local variations of the magnetic properties in Co-based multilayer films are far from the Gaussian (or Lorentzian) distribution. The asymmetric distribution could be well analyzed by a theoretical function: the lower bound of the distribution was ascribed to the finite wall-motion speed compared with the field-sweeping time, while the higher bound was ascribed to the domain coalescence. We find that all magnetic properties correlate locally with each other and a thermally activated magnetization reversal process takes place, respectively, on local regions of a submicrometer scale in ferromagnetic thin films.

ACKNOWLEDGMENT

This work was supported by the Korean Ministry of Science and Technology through the Creative Research Initiatives Project.

[1] M. Speckmann, H.P. Oepen, and H. Ibach, Phys. Rev. Lett. **75**, 2035 (1995).
[2] P. Haibach, M. Huth, and H. Adrian, Phys. Rev. Lett. **84**, 1312 (2000).
[3] S.-B. Choe and S.-C. Shin, Phys. Rev. B **62**, 8646 (2000); **59**, 142 (1999).
[4] J. Ferré, V. Grolier, P. Meyer, S. Lemerle, A. Maziewski, E. Stefanowicz, S.V. Tarasenko, V.V. Tarasenko, M. Kisielewski, and D. Renard, Phys. Rev. B **55**, 15 092 (1997).
[5] G. Bertotti, *Hysteresis in Magnetism* (Academic Press, San Diego, 1998), Pt. IV.
[6] M. Mansuripur, *The Physical Principles of Magneto-Optical Recording* (Cambridge University Press, Cambridge, England, 1995), Chap. 15.
[7] J.L. Simonds, Phys. Today **48** (4), 26 (1995).
[8] K.M. Krishnan, MRS Bull. **20** (11), 24 (1995).
[9] G.A. Prinz, Science **282**, 1660 (1998).
[10] E. Dan Dahlberg and J.-G. Zhu, Phys. Today **48** (4), 34 (1995).
[11] M.R. Scheinfein, J. Unguris, M.H. Kelley, D.T. Pierce, and R.J. Celotta, Rev. Sci. Instrum. **61**, 2501 (1990).
[12] H. Poppa, E. Bauer, and H. Pinkvos, MRS Bull. **20** (11), 38 (1995).
[13] E. Betzig *et al.*, Appl. Phys. Lett. **61**, 142 (1992).
[14] R. Wiesendanger, H.-J. Güntherodt, G. Güntherodt, R.J. Gambino, and R. Ruf, Phys. Rev. Lett. **65**, 247 (1990).
[15] R.P. Cowburn, D.K. Koltsov, A.O. Adeyeye, and M.E. Welland, Appl. Phys. Lett. **73**, 3947 (1998).
[16] T. Aign, P. Meyer, S. Lemerle, J.P. Jamet, J. Ferré, V. Mathet, C. Chappert, J. Gierak, C. Vieu, F. Rousseaux, H. Launois, and H. Bernas, Phys. Rev. Lett. **81**, 5656 (1998).
[17] J.-P. Jamet, S. Lemerle, P. Meyer, J. Ferré, B. Bartenlian, N. Bardou, C. Chappert, P. Veillet, F. Rousseaux, D. Decanini, and H. Launois, Phys. Rev. B **57**, 14 320 (1998).
[18] S.-B. Choe and S.-C. Shin, Phys. Rev. B **57**, 1085 (1998); Appl. Phys. Lett. **70**, 3612 (1997).
[19] H. Kronmüller, Phys. Status Solidi B **144**, 385 (1987).
[20] W.B. Zeper, H.W.V. Kesteren, B.A.J. Jacobs, H.M. Spruit, and P.F. Carcia, J. Appl. Phys. **70**, 2264 (1991).
[21] S. Hashimoto, Y. Ochiai, and K. Aso, J. Appl. Phys. **67**, 4429 (1990).
[22] B. Raquet, R. Mamy, and J.C. Ousset, Phys. Rev. B **54**, 4128 (1996).
[23] J. Pommier, P. Meyer, G. Pénissard, J. Ferré, P. Bruno, and D. Renard, Phys. Rev. Lett. **65**, 2054 (1990).
[24] A. Kirilyuk, J. Ferré, V. Grolier, J.P. Jamet, and D. Renard, J. Magn. Magn. Mater. **171**, 45 (1997).
[25] S.-B. Choe and S.-C. Shin, Phys. Rev. Lett. **86**, 532 (2001); Appl. Phys. Lett. **78**, 1430 (2001).
[26] L. Neél, Ann. Geophys. (C.N.R.S.) **5**, 99 (1949).
[27] W.F. Brown, Phys. Rev. **130**, 1677 (1963).